

# HEEGAARD FLOER HOMOLOGY AND ALTERNATING KNOTS

PETER OZSVÁTH AND ZOLTÁN SZABÓ

ABSTRACT. In [23] we introduced a knot invariant for a null-homologous knot  $K$  in an oriented three-manifold  $Y$ , which is closely related to the Heegaard Floer homology of  $Y$  (c.f. [21]). In this paper we investigate some properties of these knot homology groups for knots in the three-sphere. We give a combinatorial description for the generators of the chain complex and their gradings. With the help of this description, we determine the knot homology for alternating knots, showing that in this special case, it depends only on the signature and the Alexander polynomial of the knot (compare [24]). Applications include new restrictions on the Alexander polynomial of alternating knots.

## 1. INTRODUCTION

In [23] we introduced a “knot filtration” on the Heegaard Floer homology of a three-manifold  $Y$  which is induced from a null-homologous knot  $K$  in  $Y$ . (Some version of this has been independently discovered by Rasmussen, see [24].) In its most general form, this gives a  $\mathbb{Z} \oplus \mathbb{Z}$ -filtration on  $CF^\infty(Y)$ : specifically, the filtered chain homotopy type of this complex which is a knot invariant. It is sometimes more convenient to think of the induced  $\mathbb{Z}$ -filtration on  $\widehat{CF}(Y)$ . The homology of the associated graded object is a knot invariant whose Euler characteristic is the Alexander polynomial of the knot.

We consider here these invariants in the case where the ambient three-manifold is the three-sphere. We work with a suitable Heegaard diagram compatible with a planar projection of the knot. Correspondingly, we describe the “classical” aspects of the Floer theory – generators of the knot complex, their filtration levels, and absolute gradings – in terms of combinatorics of a (generic) knot projection to the plane (though the differentials in the knot complex still elude such a description). With this combinatorial description in hand, we are able to completely determine the Heegaard Floer homology for alternating knots – i.e. those for which the crossing types alternate between overcrossings and undercrossings – and give some topological applications. More calculations based on these descriptions will be given in a future paper.

**1.1. Classical Floer data for classical knots.** Let  $K \subset S^3$  be a knot. Recall that for each Heegaard diagram for the knot, we obtain a set of generators  $X$ , together with a function

$$\mathcal{F}: X \longrightarrow \mathbb{Z}.$$

The knot homology groups are homology groups of a chain complex which is freely generated by  $X$ , and the boundary maps are given by counting certain holomorphic disks. This chain complex admits a splitting

$$\widehat{CFK}(S^3, K) = \bigoplus_{\{i \in \mathbb{Z}\}} \widehat{CFK}(S^3, K, i),$$

where  $\widehat{CFK}(S^3, K, i)$  is the subcomplex generated by elements  $\mathbf{x} \in X$  with  $\mathcal{F}(\mathbf{x}) = i$ . We will call  $\mathcal{F}(\mathbf{x})$  the filtration level of the generator  $\mathbf{x}$ . There is another function

$$\text{gr}: X \longrightarrow \mathbb{Z}$$

which induces the grading on  $\widehat{CFK}(S^3, K)$ .

In fact, given a knot projection for  $K$ , and a reference point on the knot, there is a natural choice of Heegaard diagram (see Section 2). This allows us to describe the generators  $X$  and the functions  $\mathcal{F}$  and  $\text{gr}$  in terms of the knot projection.

For the description of the generators, we use the notion of *states* introduced by Kauffman for the Alexander polynomial, see [12]. We recall this briefly here.

Let  $K \subset S^3$  be an oriented knot. A generic projection of  $K$  gives a planar graph  $G$  where the vertices of  $G$  correspond to the double-points of the projection of  $K$ . Since  $G$  is four-valent, there are four distinct quadrants (bounded by edges) emanating from each vertex, each of which is a corner of some Jordan region of  $S^2 - G$ .

Let  $m$  denote the number of vertices. Clearly,  $G$  divides  $S^2$  into  $m + 2$  regions. We distinguish two of these regions which share an edge, denoting them  $A$  and  $B$ .

**Definition 1.1.** *A state (c.f. [12]) is an assignment which associated to each vertex of  $G$  one of the four in-coming quadrants, so that:*

- *the quadrants associated to distinct vertices are subsets of distinct regions in  $S^2 - G$*
- *none of the quadrants is a corner of the distinguished regions  $A$  or  $B$ .*

It is easy to see that a state sets up a one-to-one correspondence between vertices of  $G$  and the regions of  $S^2 - G - A - B$ . There is a very simple description of states in graph-theoretic terms (see also [12]). The regions in the complement of the planar projection can be colored black and white in a chessboard pattern, by the rule that any two regions which share an edge have opposite color. There is then an associated “black graph”, whose vertices correspond to the regions colored black, and whose edges correspond to vertices in  $G$ , which connect the opposite black regions. In these terms, states are in one-to-one correspondence with the maximal subtrees of the black graph (under a correspondence which associates to a state  $x$  the union of vertices of  $G$ , thought of now as edges in the black graph, to which  $x$  associates a black quadrant).

One can associate to a state a filtration level according to the following rule.

The orientation on the knot  $K$  associates to each vertex  $v \in G$  a distinguished quadrant whose boundary contains both edges which point towards the vertex  $v$ . We

call this the quadrant which is “pointed towards” at  $v$ . There is also a diagonally opposite region which is “pointed away from” (i.e. its boundary contains the two edges pointing away from  $v$ ). We define a local  $\text{Spin}^c$  structure contribution of  $x$  at  $v$  by the following rule (illustrated in Figure 2), where  $\epsilon(v)$  denotes the sign of the crossing (which we recall in Figure 1):

$$2\epsilon(v)s(x, v) = \begin{cases} 1 & x(v) \text{ is the quadrant pointed towards at } v \\ -1 & x(v) \text{ is the quadrant away from at } v \\ 0 & \text{otherwise.} \end{cases}$$

The filtration level associated to a state, then, is given by the sum

$$S(x) = \sum_{v \in \text{Vert}(G)} s(x, v).$$

Not surprisingly, this is also the  $T$ -power for the state which one encounters when calculating the Alexander polynomial, see [1], [12].

There is another integer associated to a state, called its grading, which is obtained by adding up local grading contributions at each vertex. These local contributions are non-zero on only one of the four quadrants – the one which is pointed away from at



FIGURE 1. **Crossing conventions.** Crossings of the first kind are assigned  $+1$ , and those of the second kind are assigned  $-1$ .



FIGURE 2. **Local filtration level contributions  $s(x, v)$ .** We have illustrated the local contributions of  $s(x, v)$  for both kinds of crossings. (In both pictures, “upwards” region is the one which the two edges point towards.).

$v$ . At this quadrant, the grading contribution is minus the sign  $\epsilon(v)$  of the crossing, as illustrated in Figure 3.

Accordingly, we let the grading  $M(x)$  of a state  $x$  be given by the formula

$$M(x) = \sum_{v \in \text{Vert}(G)} m(x, v).$$

With these objects in place, we can now state the following:

**Theorem 1.2.** *Let  $K$  be a knot in the three-sphere, with knot projection  $K$ . Then, there is a Heegaard diagram for the knot with the property that the knot complex  $\widehat{CFK}(S^3, K)$  is freely generated by states. Moreover, if  $\mathbf{x}$  denotes the generator of  $\widehat{CFK}(S^3, K)$  and  $x$  is its corresponding state, then  $\mathcal{F}(\mathbf{x}) = S(x)$  and  $\text{gr}(\mathbf{x}) = M(x)$ .*

**1.2. Heegaard Floer homology for alternating knots.** In the special case where the knot is alternating, Theorem 1.2 easily determine the knot homology completely in terms of the Alexander polynomial  $\Delta_K$  of the knot  $K$  and its signature  $\sigma(K)$ . (We will use the sign conventions according to which the left-handed trefoil has signature 2, c.f. [16].)

**Theorem 1.3.** *Let  $K \subset S^3$  be an alternating knot in the three-sphere, and write its symmetrized Alexander polynomial as*

$$\Delta_K = a_0 + \sum_{s>0} a_s (T^s + T^{-s}).$$

*Then,  $\widehat{HFK}(S^3, K, s)$  is supported entirely in dimension  $s + \frac{\sigma}{2}$ , and indeed*

$$\widehat{HFK}(S^3, K, s) \cong \mathbb{Z}^{|a_s|}.$$

It is very suggestive to compare the above result with the corresponding theorem of Lee on the Khovanov homology for alternating knots (see [15], see also [14], [2], [9]). The method of proof allows us to determine the full knot invariant, and hence  $HF^+$  for the zero-surgery on the knot. In particular, we obtain the following result, which is a generalization of a theorem of Rasmussen (see [24]) which calculates the Heegaard Floer



FIGURE 3. **Local grading contributions  $m(x, v)$ .** We have illustrated the local contribution of  $m(x, v)$ .

homology of three-manifolds obtained as integer surgeries along two-bridge knots. (In effect, the method of proof shows that alternating knots are “perfect” in Rasmussen’s sense.)

In the following statement, we let  $\mathcal{T}_k^+$  denote the graded  $\mathbb{Z}[U]$ -module which is abstractly isomorphic to  $\mathbb{Z}[U, U^{-1}]/\mathbb{Z}[U]$ , graded so that its bottom-most homogeneous generator has degree  $k$ . We also let the  $t_s(K)$  denote the torsion coefficients of for a knot  $K$ , i.e.

$$t_s(K) = \sum_{j=1}^{\infty} j a_{|s|+j}$$

(where the  $a_s$  are the coefficients of the Alexander polynomial of  $K$ ). Finally, for  $\sigma \in 2\mathbb{Z}$ , we let  $\delta(\sigma, s)$  be the integer defined by

$$(1) \quad \delta(\sigma, s) = \max(0, \lceil \frac{|\sigma| - 2|s|}{4} \rceil).$$

Note that  $\delta(\sigma, s)$  is the  $s^{\text{th}}$  torsion coefficient of the  $(2, |\sigma| + 1)$  torus knot.

**Theorem 1.4.** *Let  $K$  be an alternating knot, oriented so that  $\sigma(K) \leq 0$ , and let  $S_0^3(K)$  denote the three-manifold obtained by zero-surgery on  $K$ . Then,*

- for all  $s > 0$ , we have a  $\mathbb{Z}[U]$ -module isomorphism

$$HF^+(S_0^3(K), s) \cong \mathbb{Z}^{b_s} \oplus \mathbb{Z}[U]/U^{\delta(\sigma, s)},$$

where the first summand is supported in degree  $s + \frac{\sigma}{2} \pmod{2}$ , while the second summand has odd parity, and  $\delta(\sigma, s)$  is defined as in Equation (1),

- for  $s = 0$ , we have an isomorphism of graded  $\mathbb{Z}[U]$  modules

$$HF^+(S_0^3(K)) \cong \mathbb{Z}^{b_0} \oplus \mathcal{T}_{-1/2}^+ \oplus \mathcal{T}_{-2\delta(\sigma, 0) + \frac{1}{2}}^+$$

and the cyclic summand  $\mathbb{Z}^{b_0}$  lies in degree  $\frac{\sigma-1}{2}$ .

Thus, in both cases,  $b_s$  is given by the formula

$$(2) \quad (-1)^{s+\frac{\sigma}{2}} b_s = \delta(\sigma, s) - t_s(K).$$

In fact, Theorem 1.4 is a formal consequence of Theorem 1.3 (for any knot which satisfies the conclusion of Theorem 1.4, the conclusion of Theorem 1.3 holds). In fact, there are some non-alternating knots which satisfy the conclusion of Theorem 1.4. An example is given in Section 4.

**1.3. Applications to the topology of alternating knots.** We now describe some of the consequences of the above calculations for alternating knots, combined with other results on Heegaard Floer homology.

As a first consequence, we obtain the following calculation of the “correction terms” for three-manifolds obtained as surgery on  $S^3$  along  $K$ , for any alternating knot  $K$ . For the definition of the correction term in this setting, see [19]; this number is the analogue of the gauge-theoretic invariant of Frøyshov introduced in [7]. If  $Y$  is an

integer homology three-sphere then there is an associated integer  $d(Y)$  which constrains the intersection forms of four-manifolds which bound  $Y$ . We have the following result (compare [24], [8]):

**Corollary 1.5.** *Let  $K \subset S^3$  be an alternating knot, then*

$$d(S_1^3(K)) = 2 \min(0, -\lceil \frac{-\sigma(K)}{4} \rceil).$$

Theorem 1.4 can be used to give restrictions on the Alexander polynomials of alternating knots. A classical result of Crowell and Murasugi (see [4] and [17]) states that the coefficients of the Alexander polynomial for such a knot alternate in sign (indeed, the sign of  $a_s$  is  $(-1)^{s+\frac{\sigma}{2}}$ ). Theorem 1.4 in turn immediately gives the following inequality for the torsion coefficients, which is easily seen to generalize this alternating phenomenon:

**Corollary 1.6.** *Let  $K$  be an alternating knot in the three-sphere. Then for all  $s \in \mathbb{Z}$ , we have that*

$$(-1)^{s+\frac{\sigma}{2}}(t_s(K) - \delta(\sigma, s)) \leq 0,$$

where  $\delta(\sigma, s)$  are the constants defined in Equation (1).

For example, consider the knot  $K = 9_{42}$ . This knot has

$$\sigma(K) = 2 \quad \text{and} \quad \Delta_K(T) = -1 + 2(T + T^{-1}) - (T^2 + T^{-2}),$$

i.e. its Alexander polynomial is alternating, but it fails to satisfy the conditions of Corollary 1.6, so it is not alternating. (Note this was known via other means.)

Other restrictions on the Alexander polynomials of alternating knots have been conjectured by Fox, see [6] (see also [18], where these properties are verified for a large class of alternating knots). Specifically, Fox conjectures that for an alternating knot, the absolute values of the coefficients of the Alexander polynomial  $|a_s|$  are non-increasing in  $s$ , for  $s \geq 0$ . It is easy to see that the above corollary verifies Fox's conjecture for alternating knots of genus 2. For a general alternating knot, the inequalities stated above for coefficients  $s < g - 1$  are independent of Fox's prediction. However, for the first coefficient change, i.e. when  $s = g - 1$ , the above inequalities translate to the following stronger bound:

$$|a_{g-1}| \geq 2|a_g| + \begin{cases} -1 & \text{if } |\sigma| = 2g \\ 1 & \text{if } |\sigma| = 2g - 2 \\ 0 & \text{otherwise.} \end{cases}$$

Finally, we have a relationship with contact geometry. Recall that a fibered knot  $K \subset S^3$  endows  $S^3$  with an open book decomposition, and hence a contact structure, using a construction of Thurston and Winkelnkemper, see [25]. One can ask which contact structure this is.

For this purpose, recall that a contact structure in  $S^3$  has a classical invariant, the “Hopf invariant” of the induced two-plane field  $h(\xi) \in \mathbb{Z}$ , which is an integer which uniquely specifies the homotopy class of  $\xi$ . This number is defined by

$$4h(\xi) = c_1(k)^2 + 2 - 2\chi(W) - 3\sigma(W),$$

where  $W$  is any almost-complex four-manifold which bounds  $S^3$  so that the induced complex tangencies on its boundary coincide with  $\xi$ ,  $k$  is the canonical class of the almost-complex structure,  $\chi(W)$  is the Euler characteristic of  $W$ , and  $\sigma(W)$  is its signature.

Using results on the knot homology of fibered knots described in [22] (which, in turn, are based on the important work of Giroux [10]), we obtain the following:

**Corollary 1.7.** *Let  $K \subset S^3$  be an alternating, fibered knot of genus  $g$ , and let  $\xi_K$  denote its induced contact structure over  $S^3$ . Then,*

$$(3) \quad h(\xi_K) = -\frac{\sigma(K)}{2} - g(K).$$

*Moreover, the induced contact structure on  $S^3$  is tight if and only if  $h(\xi_K) = 0$ .*

In [5], Eliashberg classifies contact structures over  $S^3$ , showing that for each non-zero integer  $i$ , there is a unique contact structure  $\xi_i$  whose Hopf invariant is  $i$ , while there are two contact structures with vanishing Hopf invariant: the “standard” (tight) contact structure, and another (overtwisted) one. Combining Corollary 1.7 with Eliashberg’s classification, we obtain the following:

**Corollary 1.8.** *The standard contact structure and all other contact structures in  $S^3$  with negative Hopf invariant are precisely those contact structures which are represented by alternating, fibered knots.*

**1.4. Alternating links.** Theorem 1.3, together with many of its consequences, admits a straightforward generalization to the case of non-split, alternating links. We state and prove the generalization in Section 4. As an illustration, we use this as a stepping-stone for a calculation of the knot homology for a non-alternating knot,  $9_{48}$ .

**Acknowledgements.** The authors wish to warmly thank Jacob Rasmussen and András Stipsicz for interesting conversations.

## 2. PROOF OF THEOREM 1.2.

We prove here the state-theoretic interpretation of the classical Floer data of a knot projection stated in Theorem 1.2. The main ingredient is a Heegaard diagram which is naturally associated to a knot projection. (Note that this is not the usual diagram induced from placing the knot into “bridge position”.) We describe this Heegaard diagram presently.

Let  $K$  be a knot in  $S^3$ , and let  $G$  be a planar projection of  $K$  with  $m$  crossings. Let  $A$  denote the unbounded region in  $\mathbb{R}^2 - G$ , and we specially mark an edge  $e$  in the projection  $G$  which is contained in the closure of  $A$ . With this done, we can now construct a Heegaard diagram for  $(S^3, K)$  as follows.

Let  $B$  denote the other regions which contain the edge  $e$ , where we think of  $A$  as the “infinite region.” Let  $\Sigma$  be the boundary of a regular neighborhood in  $S^3$  of  $G$  (i.e. it is a surface of genus  $n + 1$ ); we orient  $\Sigma$  as  $\partial(S^3 - \text{nd}(G))$ . We associate to each region  $r \in R(G) - A$ , an attaching circle  $\alpha_r$  (which follows along the boundary of  $r$ ). To each crossing  $v$  in  $G$  we associate an attaching circle  $\beta_v$  as indicated in Figure 4. In addition, we let  $\mu$  denote the meridian of the knot, chosen to be supported in a neighborhood of the distinguished edge  $e$ .

Each vertex  $v$ , is contained in four (not necessarily distinct) regions. Indeed, it is clear from Figure 4, that in a neighborhood of each vertex  $v$ , there are four intersection points of  $\beta_v$  with circles corresponding to these four quadrants. Moreover, the circle corresponding to  $\mu$  meets the circle  $\alpha_B$  in a single point (and is disjoint from the other circles). It is easy to see that for any marked point  $m \in \mu$ , this construction gives a marked Heegaard diagram for  $K$  (c.f. [23]).

The correspondence between states and generators for the knot complex  $\widehat{CFK}(S^3, K)$ ,  $\mathbb{T}_\alpha \cap \mathbb{T}_\beta$ , should now be clear: an intersection point gives at each vertex (i.e.  $\beta$ -curve) one of four quadrants (corresponding, to the up to four  $\alpha$ -curves). Moreover, since the meridian  $\mu$  meets exactly one  $\alpha$ -curve, the curve corresponding to the region  $B$ , that corresponding  $\alpha$ -curve is not assigned to any of the vertices.

Before turning to the other aspects of Theorem 1.2, we recall a very useful technical device: the “Clock Theorem” of Kauffman.

**Definition 2.1.** *Two distinct elements  $x, y \in X$  are said to differ by a transposition if there is a pair of vertices  $v_1$  to  $v_2$  with the property that:*

- $x|_{G-v_1-v_2} \equiv y|_{G-v_1-v_2}$ ,
- *there is a straight path  $P$  from  $v_1$  to  $v_2$  (i.e. a path which follows along the knot  $K$ ) which does not contain the distinguished edge, so that  $x(v_1)$  and  $y(v_1)$  are the two quadrants which contain the first edge in  $P$ , and  $x(v_2)$  and  $y(v_2)$  are the two quadrants which contain the last edge in  $P$ .*

**Theorem 2.2.** (Kauffman) *Any two distinct states  $x$  and  $y$  can be connected by a sequence of transpositions.*



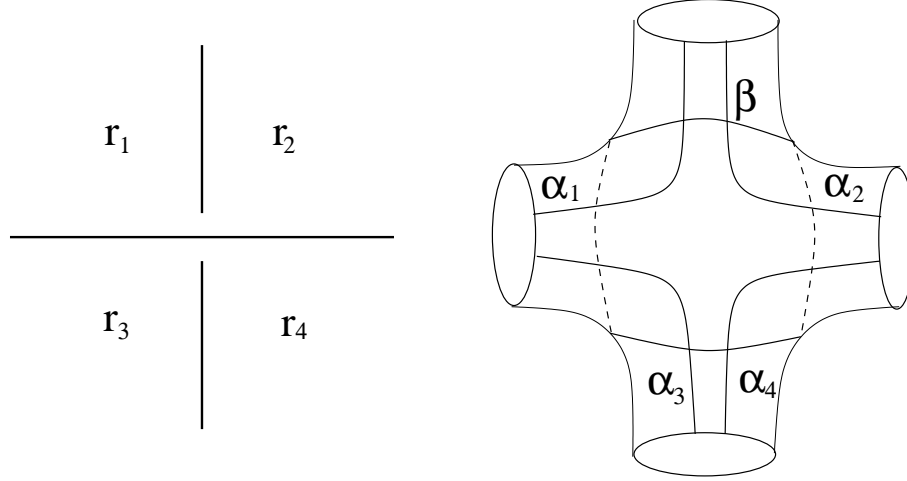


FIGURE 4. **Special Heegaard diagram for knot crossings.** At each crossing as pictured on the left, we construct a piece of the Heegaard surface on the right (which is topologically a four-punctured sphere). The curve  $\beta$  is the one corresponding to the crossing on the left; the four arcs  $\alpha_1, \dots, \alpha_4$  will close up. (Note that if one of the four regions  $r_1, \dots, r_4$  contains the distinguished edge  $e$ , its corresponding  $\alpha$ -curve should *not* be included). Note that the Heegaard surface is oriented from the outside.

The proof of the above result can be found in Chapter 2 of [12].

We now establish some lemmas used in the proof of Theorem 1.2.

**Lemma 2.3.** *Suppose that  $x, y \in X$  differ by a transposition, then the filtration difference between  $x$  and  $y$  is given by  $S(x) - S(y)$ .*

**Proof.** Orient the edge between  $v_1$  and  $v_2$  as it appears in the knot. There are now four cases, according to whether  $v_1$  or  $v_2$  are under- or over-crossings.

Suppose that the edge takes us from under-crossing at  $v_1$  to an over-crossing at  $v_2$  (i.e. our edge is on the bottom at  $v_1$  and on the top at  $v_2$ ). In this case, we claim that after possibly switching the roles of  $\mathbf{x}$  and  $\mathbf{y}$ , we can find a homotopy class  $\phi \in \pi_2(\mathbf{x}, \mathbf{y})$ , with  $n_w(\phi) = 0$  and  $n_z(\phi) = 1$ . Indeed, the domain associated to  $\phi$ ,  $\mathcal{D}(\phi)$ , has all local multiplicities zero or one; topologically, it is a surface with a collection of circle boundary components. Assume for a moment that there are no intermediate crossings between  $v_1$  and  $v_2$ . In this case, the topology of  $\mathcal{D}(\phi)$  is given as follows: the genus of  $\mathcal{D}(\phi)$  is given by the number of vertices encountered twice between  $v_2$  and the final point, it has one boundary component corresponding to the meridian  $\mu$ , it has one boundary circle for each vertex encountered only once between  $v_2$  and the final point (the corresponding  $\beta$ -circle), and there is one final boundary component (with four distinguished corner points) which is formed from arcs in  $\beta_{v_1}, \beta_{v_2}$ , and the two  $\alpha$ -curves corresponding to the

two regions which contain the edge from  $v_1$  to  $v_2$ . This is pictured in Figure 5. In the case where there are intermediate crossings between  $v_1$  and  $v_2$ , the surface looks much the same, except that now there are additional circle components, one corresponding to each compact region in the complement in  $\mathbb{R}^2$  of the part of the projection between  $v_1$  and  $v_2$  (or equivalently, one for each vertex between  $v_1$  and  $v_2$ ). Specifically, these circle components are the  $\alpha$ -curves of these intermediate regions.

The detailed description of the topology of  $\mathcal{D}(\phi)$  is not particularly relevant to the proof of the present lemma (though it is relevant in the proof of the next one); all we need here is the fact that  $n_w(\phi) = 0$  and  $n_z(\phi) = 1$ , from which it follows immediately that  $\mathcal{F}(\mathbf{x}) - \mathcal{F}(\mathbf{y}) = 1$ . From the definition of  $S(x)$ , it follows easily that  $S(x) - S(y) = 1$  (i.e. independent of the orientation on the two pieces of  $K$  transverse to our edge at  $v_1$  and  $v_2$ ) as well, verifying the lemma in this case.

Suppose that both  $v_1$  and  $v_2$  are under-crossings. When there are no intermediate intersection points between  $v_1$  and  $v_2$ , it is easy to find a square  $\phi \in \pi_2(\mathbf{x}, \mathbf{y})$  with  $n_w(\phi) = n_z(\phi) = 0$ , supported on the region of the Heegaard surface corresponding to the edge, as pictured in Figure 5. In particular, the filtration difference is zero. When there are intermediate intersection points, the region  $\phi$  now is a square with a finite number of circles removed, but it is still disjoint from  $w$  and  $z$ . Now, it is easy to see that the formula  $S(x) - S(y)$  gives zero, independent of the crossing signs of the two vertices.

The remaining two cases (where  $v_2$  is an over-crossing) are handled similarly.  $\square$

**Lemma 2.4.** *Suppose that  $\mathbf{x}$  and  $\mathbf{y}$  are a pair of intersection points, and suppose that the corresponding vertex assignments  $x$  and  $y$  in  $X$  differ by a transposition, at distinguished vertices  $v_1$  and  $v_2$ . Then, the absolute value of the difference in grading between  $\mathbf{x}$  and  $\mathbf{y}$  is one. More precisely, if  $\mathbf{x}$  is represented by light dots in Figure 6, and  $\mathbf{y}$  is represented by the dark ones, then  $\text{gr}(\mathbf{x}) - \text{gr}(\mathbf{y}) = 1$ .*

**Proof.** Domains with  $n_w(\phi) = 0$  connecting intersection points which differ by a transposition have already been demonstrated in the proof of Lemma 2.3 (see Figure 5). Our task here is to calculate their Maslov index (and, indeed, to show that it is one in all the above cases).

In all cases, we have seen that the domains  $\mathcal{D}(\phi)$  are topologically a square with a finite number of handles attached, and a finite number of disks removed. Letting  $\mathbf{x}, \mathbf{y} \in \mathbb{T}_\alpha \cap \mathbb{T}_\beta$  denote the intersection points corresponding to the states  $x$  and  $y$ , and writing  $\mathbf{x} = \{x_1, \dots, x_g\}$ , and  $\mathbf{y} = \{y_1, \dots, y_g\}$ , we have (for some numbering) that for  $i = 3, \dots, g$ ,  $x_i = y_i$ , while  $x_1, y_1, x_2$ , and  $y_2$  are the four corner points of the square. Now, in the interior of each handle attached to the square, we have a point  $x_i$  (for  $i > 2$ ), while on each circle we have a point  $x_i$ , and all the other intersection points  $x_i$  (with  $i > 3$ ) lie in the exterior of  $\mathcal{D}(\phi)$ . Thus, these extra intersection points do not affect the Maslov index. Moreover, each of the handles can be deleted, while deleting

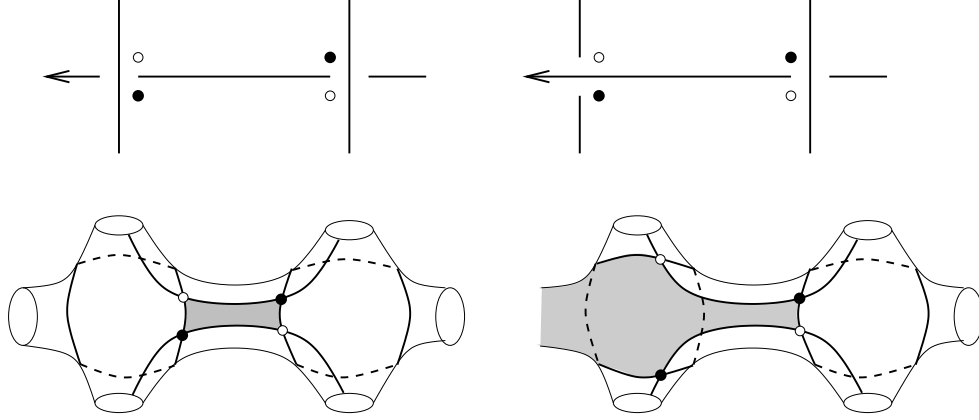


FIGURE 5. **Illustration of Lemma 2.3.** The top row represents the original projection diagram: the light circles represent the vertex assignment  $x$ , while the dark ones represent  $y$ . In the second row, we have the corresponding Heegaard picture, with the support of the homotopy class  $\phi \in \pi_2(\mathbf{x}, \mathbf{y})$  lightly shaded. (Note that there are two other cases not pictured here, but the corresponding pictures are the same as these, only viewed from underneath.)

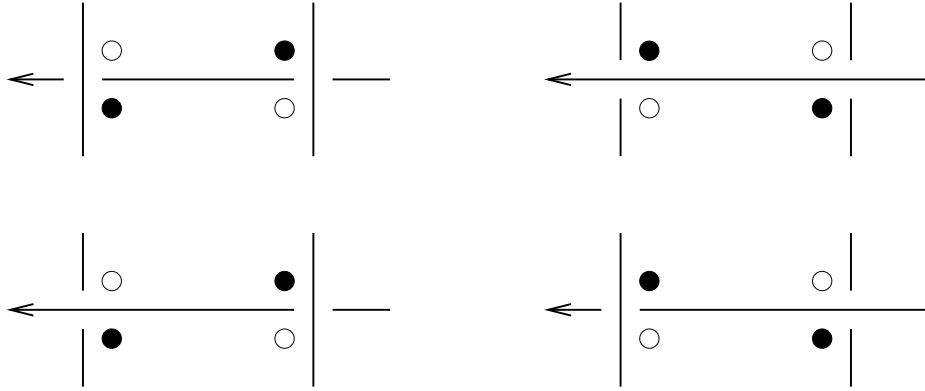


FIGURE 6. **Grading difference for intersection points which differ by a transposition.** Let  $x$  be the vertex assignment represented by the dark dots, and  $y$  be the one represented by the light ones. Then,  $\text{gr}(x) - \text{gr}(y) = 1$ .

the corresponding intersection point  $x_i$  without affecting the Maslov index. (This latter operation corresponds to destabilizing the Heegaard diagram, see [21].)

It remains then to calculate the Maslov index of a homotopy class  $\phi$  whose domain consists of square minus a finite collection of disks. We claim that for such a homotopy class,  $\mu(\phi) = 1$ . This can be seen, for example, by finding such a homotopy class in

a suitably chosen (genus  $n + 2$ ) Heegaard diagram for  $\#^{n+1}(S^1 \times S^1)$  (where here  $n$  denotes the number of disks removed). We illustrate this in the case where  $n = 1$ , in Figure 7.

□

We find it useful to introduce one more notion before proceeding to the proof of Theorem 1.2. Recall that the decoration on the knot projection (the distinguished edge, and the orientation on the knot projection) induces a natural ordering on all the edges of the knot projection. If  $v$  is any vertex in the knot projection, the *edge after*  $v$  is the last edge (in this ordering) whose closure contains  $v$ . The edge which immediately precedes it will be called the  *$v$ -penultimate edge*, and we denote it by  $e_v$ . Note also that the orientation of  $K$  and the reference point specifies an ordering on the vertices, as

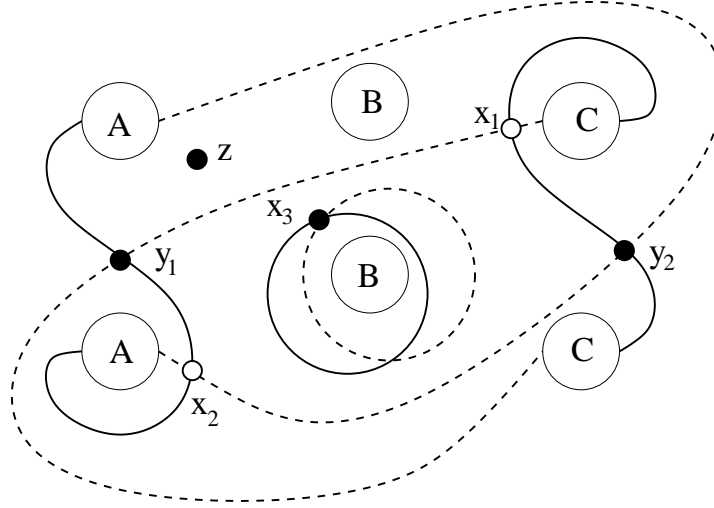


FIGURE 7. **Maslov index calculation of a square minus a disk.**

Above, we have pictured a  $g = 3$  Heegaard diagram for  $\#^2(S^2 \times S^1)$ . The dark lines represent  $\beta$ -curves, and the dashed ones represent  $\alpha$ -curves. Note that the disks labeled with capital letters  $A$ ,  $B$ , or  $C$  are to be removed, and their boundaries are pairwise identified, according to their pictured labeling. There are four intersection points in  $\mathbb{T}_\alpha \cap \mathbb{T}_\beta$ , all of which represent the  $\text{Spin}^c$  structure with trivial first Chern class. It is easy to see that  $\mathbf{x} = \{x_1, x_2, x_3\}$  and  $\mathbf{y} = \{y_1, y_2, y_3\}$  with  $y_3 = x_3$ , and basis point as chosen above. It is easy to find a domain for a Whitney disk  $\phi \in \pi_2(\mathbf{x}, \mathbf{y})$  which is a square with a disk removed. Moreover, the grading difference between these two elements is one (they are also connected by a square).

follows. We say that  $v_1 < v_2$  if the vertex  $v_1$  is crossed the second time before  $v_2$  is (on the path beginning at the reference point, following  $K$ ).

We will see that there is a *canonical state*  $x_0$  which is uniquely characterized by the property that for each crossing  $v$ ,  $x_0(v)$  is one of the two quadrants whose closure contains the edge before  $v$  (c.f. Lemma 2.5 below).

**Lemma 2.5.** *The canonical state  $x_0$  is well-defined.*

**Proof.** Let  $R(G)$  denote the set of regions in  $S^2 - G - A - B$ . Let  $X_0 = A \cup B$ . We will inductively define the canonical state  $x_0$  by finding an ordering  $v_1, \dots, v_m$  of all the vertices in the graph  $G$ , with the property that  $x_0|_{\{v_1, \dots, v_n\}}$  is uniquely defined. Correspondingly, we will exhaust  $S^2$  by a sequence of regions

$$X_0 \subset X_1 \subset \dots \subset X_m = S^2$$

with the property that  $x_0|_{\{v_1, \dots, v_n\}}$  maps onto the set of regions in  $X_n - G - X_0$  (and hence  $X_{n+1}$  is defined by attaching to  $X_n$  a region  $R_n \in R(G)$ ). In our induction hypothesis, we will assume that the  $v_i$ -penultimate is contained in the interior of  $X_i$ .

For the initial step ( $n = 0$ ),  $x_0$  is vacuously defined.

For the inductive step, either  $X_n = S^2$  (in which case we are finished), or  $X_n$  is a proper subset of  $S^2$ , in which case it must have corners, since we have assumed that our graph belongs to a knot projection. Consider the last corner point  $v_{n+1}$  of  $X_n$  (with respect to the ordering induced by the orientation on the knot). It is clear that the  $v_{n+1}$ -penultimate edge must appear in two quadrants, one of which is contained in  $X_n$ ,

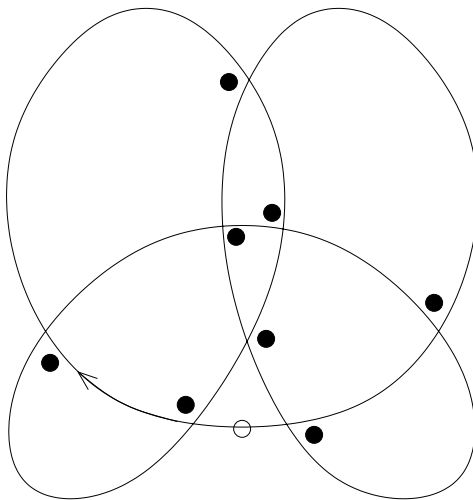


FIGURE 8. **The canonical state  $x_0$  for  $8_{16}$ .** We have illustrated here the canonical state  $x_0$  for the alternating knot  $8_{16}$ . The light circle indicates the distinguished edge, and the arrow indicates the orientation.

and the other of which is contained in a region  $R_{n+1} \subset S^2 - X_n$  (for if this hypothesis is not satisfied, we would simply be able to find a later corner vertex). It follows then that  $v_{n+1} \notin \{v_1, \dots, v_n\}$  (for the edges before all those vertices are all contained in the interiors of  $X_n$ ). We then define  $x_0(v_{n+1})$  to be the quadrant of  $R_{n+1}$  containing the  $v_{n+1}$ -penultimate edge. Let  $X_{n+1} = X_n \cup R_{n+1}$ . It is now clear from the construction of  $X_{n+1}$  that the  $v_{n+1}$ -penultimate edge is contained in the interior of  $X_{n+1}$ .

Observe that the above argument not only constructs the canonical state  $x_0$  but, since there was no ambiguity in the definition, establishes its uniqueness.  $\square$

**Proof of Theorem 1.2.** The correspondence between states and generators of  $\widehat{CFK}(S^3, K)$  in the appropriate Heegaard diagram was already explained in the beginning of this section.

To prove the assertion about filtration levels, we appeal to Lemma 2.3, which can easily be used to verify that

$$S(x) - S(y) = \mathcal{F}(\mathbf{x}) - \mathcal{F}(\mathbf{y})$$

when  $x$  and  $y$  differ by a transposition. Combining this with Kauffman's theorem, we get that  $S(x) = \mathcal{F}(\mathbf{x}) + c$ , where  $c$  is some constant which *a priori* depends on the knot projection. In particular, it follows that for some suitable choice of signs (which, of course, must coincide with the  $\mathbb{Z}/2\mathbb{Z}$  grading of the intersection point  $x$ ), the polynomial

$$\Gamma_K(T) = \sum_{x \in X(G)} (\pm 1) T^{S(x)},$$

has the form  $\Gamma(T) = T^c \cdot \Delta_K(T)$  where, as usual,  $\Delta_K(T)$  denotes the symmetrized Alexander polynomial. Indeed, the fact that  $c = 0$  follows from the fact that  $\Gamma_K(T)$  is symmetric: it coincides with the Conway-normalized Alexander polynomial, see Chapter VI of [13].

When  $x$  and  $y$  are states which differ by a transposition, it follows easily from Lemma 2.4 that  $\text{gr}(x) - \text{gr}(y) = M(x) - M(y)$ . From Kauffman's theorem, it then readily follows that there is a constant  $c$  with the property that

$$\text{gr}(x) = M(x) + c.$$

To verify that  $c = 0$ , we must show that for the canonical state  $x_0$  (whose existence was established in Lemma 2.5 above),  $M(x_0) = \text{gr}(x_0) = 0$ . Indeed, it is straightforward to see that  $M(x_0) = 0$ : the local contributions  $m(x_0, v)$  vanish for each vertex.

Finally, we see that the intersection point corresponding to  $x_0$  has vanishing absolute grading, as follows. One can reduce the Heegaard diagram for the knot described above to another Heegaard diagram for  $S^3$  by handlesliding the  $\beta$ -curves of vertices. We then arrange the  $\beta_v$ -curves in descending order, according to this ordering of the corresponding vertices, and then handleslide them “forwards” across the reference point  $z$  (but never across  $w$ ). In this manner, we obtain a new Heegaard diagram for  $S^3$ , where

the  $\beta$ -curve at any vertex  $v$  now meets only the up to two  $\alpha$ -curves corresponding to the two quadrants which contain the  $v$ -penultimate edge. Thus, the canonical state also induces an intersection point for this new Heegaard diagram, and its absolute degree agrees with the intersection point for the original Heegaard diagram (since the handleslides never crossed  $w$ ). Moreover, the uniqueness of Lemma 2.5 ensures that  $x_0$  is the only intersection point in  $\mathbb{T}_\alpha \cap \mathbb{T}_\beta$  for this new Heegaard diagram, so it must have absolute degree zero.  $\square$

## 3. RESULTS ON ALTERNATING KNOTS

For the purposes of Theorem 1.3, it is useful to have the following concrete description of the signature  $\sigma(K)$  of an alternating link, which follows work of Gordon and Litherland [11] as interpreted by Lee, see [15], which we now recall.

Consider the four quadrants meeting at some vertex  $v$ . If we orient the boundary of one of these quadrants  $Q$  (in the manner induced from the orientation of the plane), we obtain an ordering on the two consecutive edges contained in the boundary of  $Q$ . If the first of these edges is part of an “overcross” at  $v$ , we call  $Q$  an *over-first* quadrant; otherwise, we call  $Q$  an *under-first* quadrant. The alternating condition on a knot projection is equivalent to the condition that all the over-first quadrants have the same color (and hence that all the under-first ones have the other color). For definiteness, we color all the under-first quadrants white, as illustrated in Figure 9.

**Theorem 3.1.** (*Theorem 6 of [11], see also Proposition 3.3 of [15]*) *Let  $K$  be a knot with alternating projection  $G$ . Then, with the coloring conventions illustrated in Figure 9, the signature of  $K$  is calculated by the formula*

$$\sigma(K) = \#(\text{black regions in the planar projection}) - \#(\text{positive crossings}) - 1.$$

**Proof of Theorem 1.3.** Let  $x$  be any state. Glancing at the definitions of the local contributions  $m(x, v)$  and  $s(x, v)$ , one sees that

$$m(x, v) - s(x, v) + \left( \frac{\epsilon(v) + 1}{2} \right) = \begin{cases} 0 & \text{if } x(v) \text{ is an under-first quadrant} \\ \frac{1}{2} & \text{if } x(v) \text{ is an over-first quadrant.} \end{cases}$$

Adding this up over all the vertices  $v$ , and bearing in mind that the over-first quadrants are all black, and that there is exactly one black region (the distinguished one) which is not represented as  $x(v)$  for some vertex  $v$ , it follows that

$$2(M(x) - S(x)) = \#(\text{black regions in the planar projection}) - \#(\text{positive crossings}) - 1,$$

a quantity which agrees with  $\sigma(K)$ , according to Theorem 3.1. The theorem now follows immediately from Theorem 1.2.  $\square$

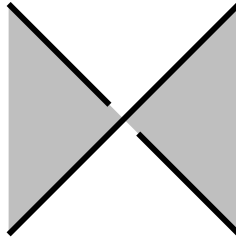


FIGURE 9. **Coloring conventions for alternating knots.** We adopt the pictured convention in the statement of Theorem 3.1.



It is straightforward if tedious to verify that in fact the previous theorem determines the filtered chain homotopy type of the knot complex uniquely in terms of the Alexander polynomial and the signature of the knot. Rather than inflicting the necessary linear algebra on our reader, we content ourselves here with the proof of Theorem 1.4. For the proof, we will use the relationship between the knot complex and the Floer homology of three-manifolds obtained by sufficiently large surgeries on  $K$ , which we recall presently.

Recall that when  $K \subset S^3$  is a knot, we have the  $(\mathbb{Z} \oplus \mathbb{Z})$ -filtered complex

$$CFK^\infty(S^3, K) = \{[\mathbf{x}, i, j] \mid \mathcal{F}(\mathbf{x}) + (i - j) = 0\}.$$

Of course, the  $\mathbb{Z} \oplus \mathbb{Z}$ -grading of  $[\mathbf{x}, i, j]$  is  $(i, j)$ , and

$$\text{gr}[\mathbf{x}, i, j] = \text{gr}(\mathbf{x}) + 2i.$$

The subcomplex where  $i \leq 0$  (or  $j \leq 0$ ) represents  $CF^-(S^3)$ , the whole complex represents  $CF^\infty(S^3)$ , and the quotient represents  $CF^+(S^3)$ . More interestingly, it is shown in [23] that for  $s > 0$ ,  $HF^+(S_0^3(K), s)$  is the homology of a finitely-generated complex

$$C(S^3, K)\{i < 0, j \geq s\} = \{[\mathbf{x}, i, j] \mid i < 0, j \geq s\}.$$

Here we have used the identification  $\text{Spin}^c(S_0^3(K)) \cong \mathbb{Z}$  given by

$$\mathfrak{s} \mapsto c_1(\mathfrak{s})/2 \in H^2(S_0^3(K); \mathbb{Z}) \cong \mathbb{Z}.$$

Indeed, this is shown to be a consequence of a theorem which identifies  $HF^+(S_n^3(K), s)$  for all sufficiently large  $n$ , with the homology of  $C(S^3, K)\{i \geq 0 \text{ or } j \geq s\}$ , shifted in degree by  $\frac{1-n}{4}$ .

**Proof of Theorem 1.4.** The proof relies on the fact, which follows from Theorem 1.3, that

$$\text{gr}(\mathbf{x}) = \mathcal{F}(\mathbf{x}) + \frac{\sigma}{2};$$

thus, for each  $[\mathbf{x}, i, j] \in CFK^\infty(S^3, K)$ ,

$$(4) \quad \text{gr}[\mathbf{x}, i, j] = i + j + \frac{\sigma}{2}.$$

We have an obvious short exact sequence

$$0 \longrightarrow C\{i < 0, j \geq s\} \longrightarrow C\{j \geq s\} \longrightarrow C\{i \geq 0, j \geq s\} \longrightarrow 0.$$

Note that  $C\{j \geq s\}$  is a chain complex which calculates  $HF^+(S^3)$ , with a shift in dimension. More precisely, the map

$$CFK(S^3, K)\{j \geq s\} \longrightarrow CFK(S^3, -K)\{i \geq 0\} \cong CF^+(S^3)$$

given by

$$[\mathbf{x}, i, j] \mapsto [\mathbf{x}, j - s, i - s]$$

is easily seen to shift grading down by  $2s$  (here,  $-K$  denotes the knot  $K$ , with opposite orientation). Now, according to Equation (4),  $C\{i \geq s, j \geq 0\}$  is a chain complex which is supported in degrees  $\geq s + \sigma/2$ . It follows immediately that

$$(5) \quad H_{\leq s + \frac{\sigma}{2} - 2}(C\{i \geq 0, j < 0\}) \cong H_{\leq s + \frac{\sigma}{2} - 2}(C\{j < s\}) \cong HF_{\frac{\sigma}{2} - s - 2}^+(S^3) = 0,$$

the latter according to our assumption that  $\sigma \leq 0$ .

To calculate  $H_*(C\{i < 0, j \geq s\})$  in the remaining degrees, we proceed similarly, now starting from the exact sequence:

$$0 \longrightarrow C\{i < 0, j < s\} \longrightarrow C\{i < 0\} \longrightarrow C\{i < 0, j \geq s\} \longrightarrow 0,$$

observing (with another application of Equation (4)) that now  $C\{i < 0, j < s\}$  is supported in degrees  $\leq s + \sigma/2 - 2$ . Letting  $Q$  denote the part of its homology in dimension  $s + \sigma/2 - 2$ , the long exact sequence in homology gives:

$$(6) \quad 0 \longrightarrow \frac{\mathbb{Z}[U]}{U^{\delta(\sigma, s)}} \cong HF_{\geq s + \frac{\sigma}{2} - 1}^-(S^3) \longrightarrow H_{\geq s + \frac{\sigma}{2} - 1}(C\{i < 0, j \geq s\}) \xrightarrow{\delta} Q \longrightarrow \dots$$

The calculation of  $HF^+(S_0^3(K), i)$  for  $i \neq 0$  is complete. Note that the isomorphism between  $C\{i < 0, j \geq s\}$  and  $HF^+(S_0^3(K), s)$  switches parity (absolute  $\mathbb{Z}/2\mathbb{Z}$  degree).

To calculate  $HF^+(S_0^3(K), 0)$ , we calculate first  $HF^+(S_n^3(K), 0)$  for all sufficiently large  $n$ .

We have the following short exact sequence

$$0 \longrightarrow C\{\max(i, j) \geq 0\} \longrightarrow C\{i \geq 0\} \oplus C\{j \geq 0\} \longrightarrow C\{\min(i, j) \geq 0\} \longrightarrow 0,$$

where  $H_*(C\{\min(i, j) \geq 0\})$  is supported in degrees  $\geq \sigma/2$ . It follows that

$$H_{\leq \frac{\sigma}{2} - 2}(C\{\max(i, j) \geq 0\}) \cong H_{\leq \frac{\sigma}{2} - 2}(C\{i \geq 0\} \oplus C\{j \geq 0\}) \cong HF_{\leq \frac{\sigma}{2} - 2}^+(S^3) \oplus HF_{\leq \frac{\sigma}{2} - 2}^+(S^3) = 0.$$

To calculate it in the remaining degrees, consider the short exact sequence

$$0 \longrightarrow C\{\max(i, j) \leq -1\} \longrightarrow C \longrightarrow C\{\min(i, j) \geq 0\} \longrightarrow 0.$$

Now,  $H_*(C\{\max(i, j) \leq -1\})$  is supported in dimensions  $\leq \sigma/2 - 2$ . Letting  $R$  denote the the part in degree  $\sigma/2 - 2$ , we have

$$0 \longrightarrow HF_{\geq \frac{\sigma}{2} - 1}^\infty(S^3) \longrightarrow H_*(C\{\min(i, j) \geq 0\}) \xrightarrow{\delta} R \longrightarrow \dots$$

It follows from this algebra, together with the results of [23] quoted before the statement of the theorem that there is a (possibly trivial) cyclic summand  $\mathbb{Z}^{b_0}$  in  $HF^+(S_n^3(K), 0)$  (for  $n$  sufficiently large) supported in dimension  $\frac{1-n}{4} + \frac{\sigma}{2} - 1$ , with the property that

$$HF^+(S_n^3(K), 0) \cong \mathcal{T}_{-2\lceil \frac{-\sigma}{4} \rceil + \frac{1-n}{4}}^+ \oplus \mathbb{Z}^{b_0}.$$

To relate this result to the Floer homology of the zero-surgery, we consider the integer surgery long exact sequence ([20], see also [19])

$$\dots \longrightarrow HF^+(S^3) \xrightarrow{F_1} HF^+(S_0^3(K)) \xrightarrow{F_2} HF^+(S_n^3(K)) \xrightarrow{F_3} \dots$$

The map  $F_3$  consists of a sum of terms, each of which decreases the absolute grading by at least  $\frac{1-n}{4}$ . It follows immediately (again, using our hypothesis that  $\sigma < 0$ ) that this map in the present case must vanish.

The map  $F_2$  now shifts degree by  $(n-3)/4$  and the map  $F_1$  shifts degree by  $-1/2$  (c.f. Lemma 7.10 of [19]), so the calculation of  $HF^+(S_0^3(K), 0)$  follows.

The only remaining piece now is the verification of Equation (2). But this follows immediately from Theorem 9.1 of [20], where the Euler characteristic of  $HF^+(Y_0)$  is identified with the torsion of  $S_0^3$ , or, more precisely, provided that  $i \neq 0$ ,

$$-t_i(K) = \chi(HF^+(S_0^3(K), i))$$

(see also [20] for the statement when  $i = 0$ ).  $\square$

We now turn to the proofs of the corollaries listed in the introduction.

**Proof of Corollary 1.6.** This is an immediate application of the theorem (after reflecting  $K$  if necessary), bearing in mind that, of course,  $b_s \geq 0$ .  $\square$

**Proof of Corollary 1.5.** In general, we have that  $d(S_1^3(K)) = d_{\frac{1}{2}}(S_0^3(K)) - \frac{1}{2}$  (see Proposition 4.12 of [19]). In the case where  $\sigma(K) \leq 0$ , the result then is an immediate application of Theorem 1.4. When  $\sigma(K) > 0$ , let  $r(K)$  denote the reflection of  $K$ ; then we have (see [19]) that

$$d_{\frac{1}{2}}(S_0^3(K)) = -d_{-\frac{1}{2}}(S_0^3(r(K))) = \frac{1}{2}$$

(with the last equation following once again from Theorem 1.4).  $\square$

For the proof of Corollary 1.7, we use the results from [22], which in turn rely on results of Giroux [10]. Specifically, if  $K \subset Y$  is a fibered knot of genus  $g$ , then  $\widehat{HFK}(-Y, K, -g) \cong \mathbb{Z}$ . The image of the generator of this group inside  $\widehat{HF}(-Y)$  is shown in [22] to depend on the knot only through its induced contact structure  $\xi_K$ , giving rise to an element  $c(\xi_K) \in \widehat{HF}(-Y)$ . Moreover, when  $Y \cong S^3$  (or, more generally, any contact structure whose induced  $\text{Spin}^c$  structure has torsion first Chern class),  $c(\xi)$  is a homogeneous element whose absolute degree of  $c(\xi)$  coincides with the Hopf invariant of  $\xi$ . Finally, in Theorem 1.4 of [22], the invariant is shown to vanishing for overtwisted contact structures.

**Proof of Corollary 1.7.** According to Theorem 1.3 the degree of an element in filtration degree  $-g$  (and hence, as above, the Hopf invariant of the induced homotopy class of two-plane field) is given by Equation (3). Note that the sign appearing in front of the signature occurs because, in the definition of  $c(\xi)$ , we reverse the orientation on the ambient three-manifold, which is equivalent to reflecting the knot.

In the case where this Hopf invariant vanishes, the induced element in  $\widehat{HF}(S^3)$  must be non-trivial, for it is the only generator in degree zero (again, according to Theorem 1.3). Thus, according to Theorem 1.4 of [22], the induced contact structure is tight.  $\square$

**Proof of Corollary 1.8.** The fact that the Hopf invariant of is non-positive, follows readily from Equation (3), together with the fact that  $|\sigma(K)| \leq 2g$ .

Moreover, we have seen in Corollary 1.7 that the overtwisted contact structure with vanishing Hopf invariant cannot be represented by an alternating knot; while it is clear that unknot represents the tight contact structure.

Finally, using Equation (3), we see that for each  $i > 0$ , the  $i$ -fold connected sum of the figure eight knot realizes the contact structure with Hopf invariant  $-i$ .  $\square$

## 4. ALTERNATING LINKS

Recall that in [23], we defined a generalization of the knot invariants  $\widehat{HFK}$  to the case of links. These link invariants satisfy a skein exact sequence (c.f. Theorem 10.2 of [23]): suppose that  $p$  is a positive crossing for a projection of a link  $L_+$ , for which both strands belong to the same component of  $L_+$ , then there is a long exact sequence (for each  $s \in \mathbb{Z}$ ) of the form:

$$(7) \quad \dots \longrightarrow \widehat{HFK}(L_-, s) \xrightarrow{f} \widehat{HFK}(L_0, s) \xrightarrow{g} \widehat{HFK}(L_+, s) \longrightarrow \dots$$

where  $L_-$  is the modified version of  $L_+$  (with a crossing-change at  $p$ ), and  $L_0$  is the resolution at  $p$  of  $L_+$ . Both maps  $f$  and  $g$  drop absolute grading by  $1/2$ , where the remaining map is non-increasing on the absolute grading.

For the following statement, recall that a link  $L$  called a *non-split, alternating link* if it has a projection which is connected, and also, if we traverse any component of  $L$ , the crossings in this projection alternate between over-crossings and under-crossings.

**Theorem 4.1.** *Let  $L \subset S^3$  be a non-split, oriented, alternating link in the three-sphere, and let  $\Delta_L$  be its Alexander-Conway polynomial. Writing*

$$(T^{-1/2} - T^{1/2})^{n-1} \cdot \Delta_L = a_0 + \sum_{s>0} a_s(T^s + T^{-s}),$$

*we have that  $\widehat{HFK}(S^3, L, s)$  is supported entirely in dimension  $s + \frac{\sigma}{2}$ , and indeed*

$$\widehat{HFK}(S^3, L, s) \cong \mathbb{Z}^{|a_s|}.$$

*Here,  $\sigma$  is the signature of the link  $L$ .*

**Proof.** Recall first that the skein exact sequence can be used to show that

$$\chi(\widehat{HFK}(S^3, L, s)) = a_i$$

(c.f. [23]).

In view of this calculation, the theorem is obtained by induction on the number of components of  $L$ , with Theorem 1.3 as base case.

For the inductive step, let  $p$  be an intersection point where two different strands of  $L$  meet. We can find two links  $L_-$  and  $L_+$  with one more intersection point  $q$ , both of which admit alternating projections, and which have the property that their resolution  $L_0$  at  $q$  is our original  $L$ . The two cases, according to the sign of the intersection point  $p$ , are illustrated in Figure 10.

When  $p$  is a positive intersection point for  $L$ , we see that (after the obvious cancellation),  $L_-$  has one fewer positive intersection points than  $L$  does, while  $L_+$  has one more positive intersection point. Moreover, the number of black regions (using the coloring conventions of Figure 9) are the same for all three links. If, on the other hand,  $p$  is a negative intersection point, then the number of black regions for  $L_-$  is one greater

than number for  $L$ , which in turn is one greater than the number for  $L_+$ . Moreover, the number of positive intersection points is the same for all three. Thus, applying Theorem 3.1, we can conclude that in either case,

$$(8) \quad \sigma(L_-) - 1 = \sigma(L) = \sigma(L_+) + 1.$$

It is now straightforward to conclude the result for  $L = L_0$  from the skein exact sequence, and the inductive hypothesis on  $L_-$  and  $L_+$ . □

Theorem 4.1 can be used to give easy generalizations to (non-split) alternating links of the results stated in the introduction for alternating knots. Rather than enumerating these, we use Theorem 4.1 to give a calculation of  $\widehat{HFK}$  for the (non-alternating) knot pictured on the left in Figure 11 (known as “9<sub>48</sub>” according to the standard knot tables, c.f. [3]).

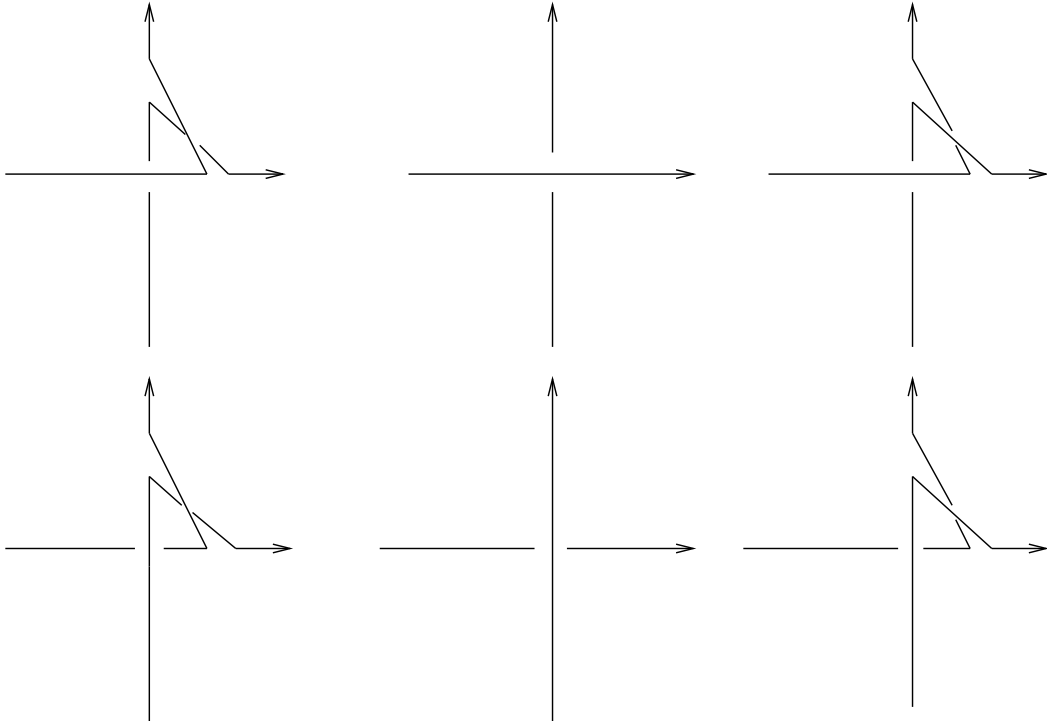


FIGURE 10. **Skein moves on alternating links.** On the left, we have two possible candidates for  $L_-$ , in the middle we have the two versions of  $L$ , while on the right we have two candidates for  $L_+$ . It is easy to see that if the links  $L$  are alternating, then the changes  $L_-$  and  $L_+$  can also be arranged to alternate (after cancelling an extra pair of intersection points, if necessary).



FIGURE 11. **The knot  $9_{48}$ .** We have illustrated this nine-crossing knot. If the crossing circled with a dotted circle is switched, we obtain the right-handed trefoil; while if the crossing is resolved, it is easy to see that we obtain the (oriented) alternating link pictured on the right.

If we change the indicated crossing, we obtain the right-handed trefoil  $K_-$ , which has

$$\begin{aligned}\sigma(K_-) &= -2 \\ \Delta_{K_-} &= T^{-1} - 1 + T.\end{aligned}$$

If the knot crossing is resolved, we obtain the two-component link  $L$  pictured on the right in Figure 11 (given the specified orientation). It is straightforward to calculate that

$$\begin{aligned}\sigma(L) &= -1 \\ (T^{-1/2} - T^{1/2}) \cdot \Delta_L &= T^{-2} - 6T^{-1} + 10 - 6T + T^2.\end{aligned}$$

It is now a straightforward application of the skein exact sequence and Theorem 4.1 that the conclusion of Theorem 4.1 holds for  $9_{48}$  (and hence also the conclusion of Theorem 1.4), even though  $9_{48}$  does not possess an alternating projection.

More calculations of knot homology groups will be given in a future paper.

## REFERENCES

- [1] J. W. Alexander. Topological invariants of knots and links. *Trans. Amer. Math. Soc.*, 30(2):275–306, 1928.
- [2] D. Bar-Natan. On Khovanov’s categorification of the Jones polynomial. *Algebraic and Geometric Topology*, 2:337–370, 2002.
- [3] G. Burde and H. Zieschang. *Knots*. Number 5 in de Gruyter Studies in Mathematics. Walter de Gruyter & Co., 1985.
- [4] R. Crowell. Genus of alternating link types. *Ann. of Math. (2)*, 69:258–275, 1959.
- [5] Y. Eliashberg. Classification of contact structures on  $\mathbf{R}^3$ . *Internat. Math. Res. Notices*, 3:87–91, 1993.
- [6] R. H. Fox. Some problems in knot theory. In *Topology of 3-manifolds and related topics (Proc. The Univ. of Georgia Institute, 1961)*, pages 168–176. Prentice-Hall, Englewood Cliffs, N.J., 1962.
- [7] K. A. Frøyshov. The Seiberg-Witten equations and four-manifolds with boundary. *Math. Res. Lett.*, 3:373–390, 1996.
- [8] K. A. Frøyshov. Equivariant aspects of Yang-Mills Floer theory. *Topology*, 41(3):525–552, 2002.
- [9] S. Garoufalidis. A conjecture on Khovanov’s invariants. Preprint, 2001.
- [10] E. Giroux. Lectures at Oberwolfach, 2001.
- [11] C. McA. Gordon and R. A. Litherland. On the signature of a link. *Invent. Math.*, 47(1):53–69, 1978.
- [12] L. H. Kauffman. *Formal knot theory*. Number 30 in Mathematical Notes. Princeton University Press, 1983.
- [13] L. H. Kauffman. *On knots*. Number 115 in Annals of Mathematics Studies. Princeton University Press, 1987.
- [14] M. Khovanov. A categorification of the Jones polynomial. math.QA/9908171, 1999.
- [15] E. S. Lee. The support of the Khovanov’s invariants for alternating knots. math.GT/0201105, 2002.
- [16] W. B. Raymond Lickorish. *An introduction to knot theory*, volume 175 of *Graduate Texts in Mathematics*. Springer-Verlag, 1997.
- [17] K. Murasugi. On the genus of the alternating knot. I, II. *J. Math. Soc. Japan*, 10:94–105, 235–248, 1958.
- [18] K. Murasugi. On the Alexander polynomial of alternating algebraic knots. *J. Austral. Math. Soc. Ser. A*, 39(3):317–333, 1985.
- [19] P. S. Ozsváth and Z. Szabó. Absolutely graded Floer homologies and intersection forms for four-manifolds with boundary. math.SG/0110170.
- [20] P. S. Ozsváth and Z. Szabó. Holomorphic disks and three-manifold invariants: properties and applications. math.SG/0105202.
- [21] P. S. Ozsváth and Z. Szabó. Holomorphic disks and topological invariants for rational homology three-spheres. math.SG/0101206.
- [22] P. S. Ozsváth and Z. Szabó. Heegaard Floer homologies and contact structures. Preprint, 2002.
- [23] P. S. Ozsváth and Z. Szabó. Holomorphic disks and knot invariants. Preprint, 2002.
- [24] J. Rasmussen. Floer homologies of surgeries on two-bridge knots. math.GT/0204056, 2002.
- [25] W. P. Thurston and H. E. Winkelnkemper. On the existence of contact forms. *Proc. Amer. Math. Soc.*, 52:345–347, 1975.



DEPARTMENT OF MATHEMATICS, COLUMBIA UNIVERSITY, NEW YORK 10027  
`petero@math.columbia.edu`

DEPARTMENT OF MATHEMATICS, PRINCETON UNIVERSITY, NEW JERSEY 08540  
`szabo@math.princeton.edu`